Permafrost and Periglacial Processes

WILEY

REVIEW ARTICLE OPEN ACCESS

Advances in Permafrost Representation: Biophysical Processes in Earth System Models and the Role of Offline Models

Heidrun Matthes[1] | Adrien Damseaux[1,2] | Sebastian Westermann[3] | Christian Beer[4] | Aaron Boone[5] | Eleanor Burke[6] | Bertrand Decharme[5] | Hélène Genet[7] | Elchin Jafarov[8] | Moritz Langer[1,9] | Frans-Jan Parmentier[3] | Philipp Porada[4] | Anna Gagne-Landmann[10] | Deborah Huntzinger[10] | Brendan M. Rogers[8] | Christina Schädel[8] | Tobias Stacke[11] | Jon Wells[10] | William R. Wieder[12]

[1]Climate Sciences, Alfred Wegener Institute Helmholtz Center for Polar and Marine Research, Potsdam, Germany | [2]Atmospheric Environmental Research, Karlsruher Institut für Technologie, Garmisch-Partenkirchen, Germany | [3]Department of Geosciences, University of Oslo, Oslo, Norway | [4]Department of Earth System Sciences, Universität Hamburg, Hamburg, Germany | [5]Centre National de Recherches Météorologiques, Météo-France, CNRS, Université de Toulouse, Toulouse, France | [6]Met Office Hadley Centre, Exeter, UK | [7]Institute of Arctic Biology, University of Alaska Fairbanks, Fairbanks, Alaska, USA | [8]Woodwell Climate Research Center, Falmouth, Massachsetts, USA | [9]Faculty of Science, Earth and Climate, Vrije Universiteit Amsterdam, Amsterdam, Netherlands | [10]School of Earth and Sustainability, Northern Arizona University, Flagstaff, Arizona, USA | [11]Climate Dynamics, Max-Planck-Institut für Meteorologie Hamburg, Hamburg, Germany | [12]Climate and Global Dynamics, National Center for Atmospheric Research, Boulder, Colorado, USA

Correspondence: Heidrun Matthes (heidrun.matthes@awi.de)

Received: 16 April 2024 | **Revised:** 6 January 2025 | **Accepted:** 16 January 2025

Funding: H.M. was supported by the European Union's Horizon 2020 Program SOCIETAL CHALLENGES (grant agreement no. 869471). T.S. was funded by the European Research Council under the European Union's Horizon 2020 research and innovation program as part of the Q-Arctic project (Grant agreement No. 951288).

Keywords: Earth system modeling | permafrost modeling | soil biogeophysical dynamics

ABSTRACT

Permafrost is undergoing rapid changes due to climate warming, potentially exposing a vast reservoir of carbon to be released to the atmosphere, causing a positive feedback cycle. Despite the importance of this feedback, its specifics remain poorly constrained, because representing permafrost dynamics still poses a significant challenge for Earth System Models (ESMs). This review assesses the current state of permafrost representation in land surface models (LSMs) used in ESMs and offline permafrost models, highlighting both the progress made and the remaining gaps.

We identify several key physical processes crucial for permafrost dynamics, including soil thermal regimes, freeze–thaw cycles, and soil hydrology, which are underrepresented in many models. While some LSMs have advanced significantly in incorporating these processes, others lack fundamental elements such as latent heat of freeze–thaw, deep soil columns, and Arctic vegetation dynamics. Offline permafrost models provide valuable insights, offering detailed process testing and aiding the prioritization of improvements in coupled LSMs.

Our analysis reveals that while significant progress has been made in incorporating permafrost-related processes into coupled LSMs, many small-scale processes crucial for permafrost dynamics remain underrepresented. This is particularly important for capturing the complex interactions between physical and biogeochemical processes required to model permafrost carbon dynamics. We recommend leveraging advancements from offline permafrost models and progressively integrating them into LSMs, while recognizing the computational and technical challenges that may arise in coupled simulations. We highlight the

importance of enhancing the representation of physical processes, including through improvements in model resolution and complexity, as this is a fundamental precursor to accurately incorporate biogeochemical processes and capture the permafrost carbon feedback.

1 | Introduction

Around 11% of the exposed land globally is underlain by permafrost, mostly in areas that face rapid changes in climate due to Arctic Amplification [1, 2]. In the last decade, permafrost temperatures have warmed almost everywhere in the circum-Arctic [3], driving substantial changes in hydrology, landscapes, biogeochemical cycles [4, 5], ecosystems and biodiversity [6], infrastructure [7–9], and general sustainability of living on permafrost [10, 11]. Arctic and subarctic soils harbor a vast reservoir of carbon, estimated to be roughly twice the amount present in Earth's atmosphere [12–15]. Presently, the majority of this carbon is locked within the permafrost. However, the ongoing effects of global warming are gradually rendering this organic matter susceptible to decomposition. As a consequence, the release of CO_2 and CH_4 emissions exacerbates temperature rises, amplifying the significance of the permafrost carbon feedback as a crucial yet uncertain terrestrial climate factor [16, 17].

The need to understand permafrost distribution as well as permafrost responses to climate change has led to a long tradition of applying numerical models to simulate permafrost extent and active layer depth (ALT). Riseborough et al. [18] supplied an overview over the application and development of spatial permafrost models, mostly stand-alone models on a regional scale, using meteorological conditions such as climate projections for the future as upper boundary conditions. They emphasized the need to incorporate the developments within these models into Global Circulation Models (GCMs). Koven, Riley and Stern [19] provide an overview of the permafrost representation in the Coupled Model Intercomparison Project Phase 5 (CMIP5) ([20]) GCMs and their trajectories for permafrost under climate change, concluding that many models fail to agree with "fundamental aspects of the observed soil thermal regime at high latitudes".

Since CMIP5, there has been an increasing awareness of the importance of the permafrost carbon feedback in the climate system. Specifically, synthesis and model investigations have suggested that the impact of permafrost thaw on greenhouse gas emissions may impact climate at the global scale (e.g., [5, 16, 17, 21]). Therefore, representing the feedback between permafrost carbon emissions and the climate system [4, 5, 22] and the interaction between permafrost and hydrology [23–25] is crucial.

Land surface representation in Earth system models (ESMs), in general, has advanced significantly over the past decades, from simple schemes producing lower boundary conditions for the atmosphere to complex land surface models (LSMs) [26]. Process representation has evolved from the basic surface energy fluxes to explicit consideration of dynamic vegetation, carbon cycling, crops, or urban areas and, very recently, even considering lateral interaction between grid cells and between landscape units [27].

In concurrence with these model improvements, various gaps have been identified that need to be addressed to make LSMs in ESMs more reliable in representing permafrost processes and their impacts and feedback on the global climate system.

The Intergovernmental Panel on Climate Change (IPCC) states that for the next assessment report, in relation to biogeochemical feedback and permafrost, we need an improved "understanding and representation in Earth system models of changes in land carbon storage and associated carbon–climate feedbacks including: better treatment of the CO_2 fertilization, nutrient-limitations, soil organic matter (SOM) stabilization and turnover; land-use change; large-scale and fine-scale permafrost carbon; plant growth, mortality, and competition dynamics; plant hydraulics; and disturbance processes." [28]. Blyth et al. [26] state that for permafrost representation in land surface modeling, the current challenges are (1) regional pedotransfer functions, (2) soil properties changing over time, (3) topography changes over time, and (4) representations of subgrid heterogeneity (e.g., soil tiling to explicitly model peat soils, variations in maximum infiltration, soil textures, and irrigation). Schädel et al. [22] emphasize that "Earth system models must include permafrost carbon processes," identifying process representations required to model permafrost carbon dynamics. They emphasize existing poor representation of lateral fluxes, snow distribution and insulation, wetland and lake distribution, and subgrid-scale heterogeneity in LSMs.

Despite the strong consensus on the important impacts of permafrost on the global climate system under climate change projections, not all models in the Coupled Model Intercomparison Project Phase 6 (CMIP6) ([29])—the latest CMIP, which informed the 6th IPCC assessment report [30]—utilize land surface schemes appropriately set up to represent permafrost dynamics. A number of studies have used the CMIP6 models to assess their capabilities in representing permafrost dynamics. Burke, Zhang, and Krinner [31] provided an extensive analysis of 18 CMIP6 models in their ability to capture present-day permafrost-related variables in terms of permafrost extent, mean annual near-surface temperature, and ALT. Two-thirds of the models analyzed accurately simulated permafrost extent within 15% of the observed range, compared to four-fifths of the models assessed in Chadburn et al. [32] for CMIP5. However, the multimodel ensemble mean from CMIP6 exhibits a smaller bias than the multimodel CMIP5 mean. Less than half of the analyzed CMIP6 models simulated ALT within the observed range, with a slight improvement over the CMIP5 models, but ALT representation of the multimodel ensemble mean between CMIP5 and CMIP6 remained the same.

Andresen et al. [23] compared eight LSMs participating in the Permafrost Carbon Network Model Intercomparison Project (PCN-MIP) ([4]) with respect to soil hydrology in the Arctic. Even though these LSMs were often used in more advanced

setups than for coupled simulations within ESMs, the study found that while most models captured the long-term timing of surface runoff from the major river basins in the northern permafrost region, the magnitude was underestimated. The IPCC itself states that from the 11 models analyzed for carbon–concentration and carbon–climate feedbacks within the 1pctCO2 simulations from the Coupled Climate-Carbon Cycle Model Intercomparison Project (C^4MIP) framework [33], only two represented permafrost carbon [28].

These previous studies focus on identifying and discussing the strengths and deficiencies of the models with respect to permafrost dynamics, mostly without explicitly discussing process representation in the models. Our review starts with presenting the physical processes that are considered important for representing permafrost dynamics in LSMs in terms of soil physics, snow-soil interactions, and snow-vegetation-soil interactions, since thermal and hydrological dynamics govern permafrost thaw and are required precursors for subsequent release of greenhouse gases. We leave an extensive discussion of biogeochemical processes to Gagné-Landmann et al. [34], which focuses on biogeochemical and biogeophysical permafrost related process representation in models with respect to permafrost carbon. This description of relevant processes is followed by describing existing implementations and parameterizations of these processes in the global LSMs used in ESMs from the CMIP6 ScenarioMIP contributions. Finally, we assess the ongoing progress in LSM developments towards integrating processes considered important for representing permafrost dynamics, including future directions in this field that are informed by advancement of standalone permafrost models, that is, those models that are not interactively coupled to an atmosphere. We aim to identify possible synergies and assess if the developments in stand-alone models could be used to stimulate advancements in LSMs in ESMs.

2 | Key Biophysical Processes for Permafrost Modeling in LSMs

The representation of permafrost dynamics depends on the soil processes and soil–snow–vegetation interactions considered in a given model. Commonly considered soil processes are vertical transport of heat and water in multilayer soil columns of often several meters in depth, including important processes for permafrost like latent heat exchange from freezing and melting ground ice, and organic matter content in the soil column. Models focused on hydrology often also consider lateral heat transport associated with lateral water flow. The exchange of water and heat with the atmosphere at the top of the soil is considered via surface characteristics and processes representing snow, vegetation, surface water, and meteorology.

2.1 | Soil Heat Conductivity

Due to its strong influence on soil thermodynamics, soil thermal conductivity is considered one of the most important physical parameters in land modeling studies [24, 35–37]. Incorporating the dependency of soil thermal conductivity on the presence of liquid water and ice is especially important in permafrost soils [38], which also points to the importance of representing soil water content correctly. Gao and Coon [39] show that neglecting the redistribution of water in partially frozen, unsaturated soils caused by increased matric suction (cryosuction) in model experiments with the Advanced Terrestrial Simulator (ATS v1.2) resulted in 10%–30% errors in thaw depth and 10%–30% errors in 1 m soil temperature. A detailed description of the soil thermal conductivity schemes for mineral soils used in the LSMs participating in CMIP6 can be found in Dai et al. [35] and He et al. [36]. He et al. [36] conclude from their comparisons with measurements of frozen soil thermal conductivity that there are clear differences in performance between the different schemes analyzed and that no scheme performs particularly well, suggesting that new approaches developed specifically for frozen soils may be needed [40]. In addition, two key requirements related to the structure of the model soil columns have been identified from previous studies. First, Lawrence et al. [41] emphasized the need for high vertical resolution within the top 3 m of the soil column to improve the representation of freezing and thawing front dynamics and ALT. Secondly, Alexeev et al. [42] demonstrated that the soil column should extend to a minimum depth of 30 m to properly resolve the seasonal cycle in temperature. A geothermal steady heat flow at depths greater than 40 m as the lower boundary condition was found acceptable to simulate long-term permafrost changes [43].

Inclusion of an upper organic layer is important and improves estimates of ALT and keeps permafrost cooler in models [44, 45]. Soil organic matter (SOM) exhibits distinct hydraulic and thermal properties when compared to mineral soils, augmenting available water capacity [46] and influencing soil porosity and saturated hydraulic conductivity [47–49]. These differences result in significantly reduced soil thermal conductivity, while concurrently elevating soil heat capacity in comparison to mineral soils, ultimately manifesting as lower temperatures during the summer months. This phenomenon has been studied over Arctic permafrost regions [48, 50–54]. At the same time, SOM increases soil field capacity and therefore soil water content after rainfall or snowmelt, and both thermal conductivity and heat capacity increase under wet conditions. This leads to an elevated heat conduction in particular in spring.

2.2 | Snow

Snow exerts a strong control over the surface energy balance that influences the soil thermal regime [55]. Snow thermal conductivity plays a pivotal role in determining the rate of heat transfer to the underlying soil, which is arguably the most crucial model parameter within snow physics [24] and one of the largest sources of uncertainty in LSMs with respect to soil temperature simulation [56]. The use of too simplistic a snow scheme can lead to an incorrect assessment of permafrost extent, and even affect the biogeochemistry [57]. Commonly, LSMs parameterize snow thermal conductivity as a function of simulated snow density or snow temperature [58]. However, the representation of snow density profiles common to tundra environments (shallow snow pack, high-density wind-slab top layer, and low-density hoar frost-dominated lowest layer) is challenging even for sophisticated snow models [54, 59], which introduces large uncertainties into the determination of snow thermal conductivity from snow densities. These

dynamics also play out seasonally. For example, an increasing depth of snow with low density in autumn counteracts the increasing heat loss into the atmosphere, which is one important factor for the pronounced zero curtain period in autumn. By comparison, snow dynamics are reversed in spring, where a longer snow cover cools permafrost. In addition, snow depth variability due to extreme temperature events in autumn can substantially reduce the insulation strength of snow, hence cooling the soil [60]. Finally, accurately simulating snow thermal properties under climate change scenarios becomes even more challenging. Projected increases in rain-on-snow events [61, 62] may have substantial consequences on soil thermal dynamics during winter, resulting from rain water infiltration through the snow layer [63].

2.3 | Vegetation

Beyond soils and snow, vegetation exerts control over the surface energy balance [64]. For permafrost ecosystems, the composition and thickness of mosses strongly reduce soil heat flux in summer [65] and may substantially decrease average soil temperature due to insulation of the surface layer in the summer months [66, 67] while heat conductivity can be increased by wet mosses and lichens [60]. Certain lichen species have a high albedo [64] and may lead to surface cooling in open canopy ecosystems [68], while shrub canopies can influence local microclimate by shading the ground in summer [69]. Tall vegetation also captures more snow in winter [70], and ecosystems with tall shrubs and trees have warmer soil temperatures than those with short-statured tundra vegetation [71]. This suggests that the ongoing greening and shrubification of the Arctic may lead to a thickening of the active layer (e.g., [72, 73]). Simultaneously, taller vegetation like shrubs, which do not get buried by snow completely, change the land surface–atmosphere energy exchange. They may lead to lower albedo in spring and autumn [74, 75]. Shrubs buried in snow are typically taken to have a warming effect on permafrost by decreasing the overall conductivity of the snowpack [76, 77], but recent results suggest that low shrubs can actually cool the ground in winter by providing a thermal bridge through the snowpack [78]. Representing a shrub vegetation type is essential for LSMs to be able to capture these dynamics, as well as an adequate representation of vegetation buried in snow. In boreal forests, Abe et al. [79] suggest from a modeling study that changes in LAI lead to changes in canopy interception of snow, affecting the snow-albedo feedback. An accurate simulation of vegetation-permafrost interactions is, therefore, not only necessary to model the exchange of carbon with the atmosphere but also to project the present and future physical state of permafrost.

2.4 | Wetlands

Wetlands, with their organic-rich soils and water-saturated conditions, play a crucial role in shaping permafrost dynamics. These environments act as insulators to the underlying permafrost, slowing the rate of thawing. However, changes in wetland water balance due to climate warming can lead to the formation or disappearance of permafrost beneath these areas. The hydrology of permafrost wetlands is complex and sensitive to climate change, as the presence of ice affects water movement and can lead to the formation of unique landforms such as polygonal tundra, as well as wetland-associated dry permafrost landforms such as palsas and peat plateaus. Open water bodies, including lakes, ponds, and rivers, also significantly influence permafrost conditions. These water bodies store heat and freeze slowly due to latent heat effects, leading to the development of taliks—unfrozen ground in permafrost areas—beneath them. This process accelerates permafrost thawing and complicates the thermal stability of permafrost. Moreover, open water bodies alter groundwater flow paths and dynamics, influencing surface water thermal regimes and stream temperatures, which are crucial for understanding the broader impacts of permafrost thaw on Arctic ecosystems. Incorporating wetlands and open water bodies into permafrost models is essential for realistic simulations of permafrost dynamics under current and future climate scenarios. Detailed data on water body distribution, size, and seasonal dynamics are necessary for accurate representation within models.

2.5 | Nongradual Thaw Processes

In addition to the gradual thaw of permafrost driven by a warming climate, abrupt thaw plays an important role for permafrost thaw-related CO_2 emissions [80]. Abrupt thaw is associated with disturbances on often small spatial scales, related to processes like permafrost-fire interactions, belowground combustion and melt of excess ground ice, subsequent subsidence, and thermokarst formation in ice-rich permafrost, as well as changes in snow cover and hydrology [81]. Moreover, nongradual disturbance processes, which largely control the rate of permafrost degradation, take place at spatial scales of a few to hundreds of meters (e.g., [82]). Among these disturbance processes, wildfires are included in some LSMs that have the capability to employ dynamic vegetation [83]; however, fires only affect vegetation, and there is no direct permafrost-fire interaction, while other listed forms of disturbance remain poorly represented [22]. In addition, in order to realistically represent the effects of disturbances like fire on vegetation structure and dynamics and associated effects on permafrost, different trajectories of plant functional type (PFT) developments are required where patches (or cohorts) are defined based on the time since a disturbance [84], a capacity only few LSMs have.

2.6 | Factors Beyond Process Representation

Besides process representation, horizontal resolution is an important feature for capturing the very high landscape heterogeneity of permafrost areas. Even ESMs using sophisticated LSMs in their framework are still relatively coarse in their horizontal resolution, with the median resolution of atmosphere and land in CMIP6 being ~140 km (ranging from 75 to 250 km, [30]). Many models attempt to address this problem by using tiling approaches to represent landscape heterogeneity, allowing for grid cell fractions of different vegetation types (primary and secondary natural vegetation, crops, etc.), lakes, glaciers, wetlands, and recently, hillslope categories [85]. However, these approaches cannot overcome the lack of high-resolution input data

for critical drivers of soil thermal regimes (e.g., soil texture map, ice content, and organic layer thickness). Furthermore, model results are dependent on parameter choices in their process representations (e.g., [86, 87]), suggesting that careful attention to parameter choices is critical to improving model accuracy and reliability.

Collectively, these challenges related to soils, snow, vegetation, disturbance, and horizontal resolution underscore the challenges of adequately simulating physical permafrost dynamics in models that are used for climate change projections.

3 | Where Do the LSMs of the CMIP6 ESMs Stand?

In our following analysis, we focus on models that have a maximum soil depth exceeding 3 m (center depth of the lowest soil layer; see comment on soil column requirements above) and accessible documentation of the representation of soil physics. We give an overview of the important physical processes in permafrost representation discussed in the previous section for the models we consider and how their approaches have been discussed in the literature. Note that contribution to CMIP6 has been an ongoing effort, many contributions occurred after the deadline for inclusion in the IPCC AR6, and many models have provided simulations with updated coupled ESMs since. This study did not track the submission dates of models to the CMIP6 archive; rather, we describe the state of model development of the current list of CMIP6 contributions to both CMIP and ScenarioMIP ([88], accessed 12 January 2024), which might yield different assessments of models compared to other studies. We restrict our analysis to the most up-to-date versions of LSMs used in the CMIP6 ESM simulations. We acknowledge the capability of LSMs to be run with different levels of complexity, for example, in the employment of deep soil columns, dynamic vegetation, and terrestrial carbon cycling. We describe the setup that was actually used in CMIP6 ScenarioMIP, in the knowledge that these settings are not necessarily employed in all model intercomparison projects and do not necessarily reflect the full capability of the LSMs with regard to processes relevant for permafrost dynamics.

Within CMIP6, 49 institutions submitted simulations from 133 models (including different model versions), 64 of which contributed to ScenarioMIP, which is focused on future projections of the Earth system under different shared socioeconomic pathways (see Table S1; [88]). These models employ 18 different LSMs (where we counted different development versions of the same LSM as one LSM for simplicity), among which we identified eight models that do not fulfill the criteria: CABLE (too shallow, center depth of lowest layer 2.9 m), BCC-AVIM2 (too shallow, 2.9 m), CLASS/CTEM (too shallow, 2.3 m), HTESSEL and HTESSEL/LPJ-GUESS (too shallow when used in the coupled setting within the EC-Earth framework, 1.95 m), GISS LSM (too shallow, 2.7 m), JULES (too shallow, 2 m), HAL 1.0 (inadequate documentation), NOAH-MP (too shallow in its standard configuration, 2 m), and INM-LND1 (inadequate documentation). The ESM MCM-UA-1-0 gives the "standard Manabe bucket hydrology scheme" as a sole description of its land component and was also excluded from further analysis. Table 1 provides an overview of these LSMs and the CMIP6 models they are used in.

Figure 1 provides an overview of the column structure of the LSMs analyzed in our study, demonstrating the different approaches with a group of models with relatively shallow columns (ISBA, GFDL-LM4, MATSIRO, and JSBACH) and a group with deep soil columns considered most suitable for long-term climate simulations (CLM5, CoLM, ELM, and ORCHIDEE), whereas Table 2 summarizes the differences in soil physics among those models, focusing on column depth and discretization, heat capacity and soil thermal conductivity, and inclusion of organic matter.

3.1 | Soil Heat Conduction

Models discussed here represent heat transport in soil with the 1D heat flow equation, including latent heat as a sink or source (with the exception of JSBACH and MATSIRO6.0), and none of the models incorporate lateral heat flow. The key differences lie in how they estimate soil heat capacity and soil thermal conductivity. Most models use a soil heat capacity scheme derived from de Vries [109] or altered after this scheme. Only GFDL-LM4 adopts a fixed soil heat capacity dependent on soil type, which may adversely impact soil temperature representation. Soil thermal conductivity parameterization schemes are employed globally, for desert, rainforest, or permafrost soils alike. While models account for freezing of the soil when calculating soil thermal conductivity, a comprehensive comparison by He et al. [36] demonstrated that all of the analyzed 39 approaches to calculate soil thermal conductivity in frozen soils performed inadequately, which suggests that new parameterizations are needed.

SOM is considered in most models, following different schemes, for example, a linear weighted combination of organic soil properties with standard mineral soil properties as suggested by Lawrence and Slater [47], sometimes with added complexity. ISBA incorporates a pedotransfer function linking soil water retention at various pressure levels to the fiber content of organic soils [48]. ISBA calculates soil thermal conductivities as geometric averages of organic and mineral soils. JSBACH does not explicitly represent SOM, alternatively representing a moss and/or lichen layer at the surface, which possesses dynamic moisture contents and thermal properties, thus serving as a physical representation of the surface organic layer [32, 66]. MATSIRO6.0 adopts a similar approach by incorporating a top organic layer [112]. There is no extensive comparison of the performance of these different schemes, but the summer offset calculated by Burke, Zhang, and Krinner [31] suggests that they are widely different in their effects.

The majority of models solve water mass transfer by using Darcy's law and soil moisture dynamics by using the Richards equations in a multilayered representation of the soil column. There are two commonly used models to calculate the relationship between volumetric water content and soil hydraulic conductivity, as well as soil matric potential: one by Brooks and Corey [116] and the other by Van Genuchten [117]. Note again that these schemes are employed globally and were not specifically developed for permafrost soils.

TABLE 1 | CMIP6 models and their respective LSMs. LSMs discussed further are marked in bold.

Land surface models (previous versions)	Earth system model(s)	Reference paper (LSM)
CTSM/CLM5 (CLM4.5, CLM4)	CESM2, CESM2-FV22, CESM2-WACCM, CIESM, CMCC-CM2-SR5, CMCC-ESM 2, FGOALS-g3, FIO-ESM-2-0, KIOST-ESM, NorESM2-LM, NorESM2-MM, SAM0-UNICON, TaiESM1	Lawrence et al. [41]
ISBA/SURFEX 8.0c	CNRM-CM6-1, CNRM-ESM 2-1	Decharme et al. [89]
ELMv1.1 (v1.0)	E3SM-1-0, E3SM-1-1, E3SM-1-1-ECA, E3SM-2-0	Golaz et al. [90]
GFDL-LM4.1 (LM4)	GFDL-CM4, GFDL-ESM 4	Zhao et al. [91], Shevliakova et al. [92]
ORCHIDEE-MICT v8.4.1	IPSL-CM6A	Guimberteau et al. [93]
JSBACH3.20 (v3.1)	MPI-ESM 1-2, AWI-CM-1-1, AWI-ESM-1, NESM3	Reick et al. [94]
MATSIRO6.0	MIROC6	Yokohata et al. [95]
CoLM	CAMS-CSM1-0, CAS-ESM 2.0	Dai et al. [96], Li et al. [97]
CLASS3.6/CTEM1.2	CanESM5	Swart et al. [98]
JULES-ES-1.0	UKESM-1-LL	Mathison et al. [99]
JULES-HadGEM3-GL7.1	HadGEM3-GC31-MM, HadGEM3-GC31-LL, KACE-1-0-G	Wiltshire et al. [100]
ICON-Land	ICON-ESM	Schneck et al. [101]
NOAH-MP	IITM-ESM	He et al. [102]
CABLE2.5 (2.4)	ACCESS-CM2, ACCESS-ESM 1-5	Haverd et al. [103]
BCC-AVIM2 (AVIM1)	BCC-CSM2-MR	Wu et al. [104]
HTESSEL/LPJ-GUESS	EC-Earth3-CC, EC-Earth-Veg	Smith et al. [105]
GISS LSM	GISS-E2-1-G, GISS-E2-2-G, GISS-E3-G	Kelley et al. [106]
HAL 1.0	MRI-ESM 2-0	Yukimoto et al. [107]
INM-LND1	INM-CM4-8, INM-CM5-0	Volodin et al. [108]

3.2 | Snow

Snow cover significantly impacts the thermal regime of the soil, but its insulating properties are highly variable and insufficiently detailed in ESMs [59, 118]. All LSMs discussed here employ multilayer snow, with some models allowing for a dynamic number of snow layers. An overview of the snow representation within the LSMs can be found in Table S2. Four models parameterize fresh snow density depending on variables like wind speed and temperature. Three models employ fixed snow densities, while the other schemes allow dynamic snow densities, considering processes like compaction due to overburden pressure, destructive metamorphism, and melt metamorphism. Constructive metamorphism [58], related to temperature gradients and the formation of depth hoar, is not included in any of the snow models studied here or in most state-of-the-art snowpack models [119]. Studies show that neglecting the role of depth hoar in providing thermal insulation properties to Arctic snow packs can have significant consequences for soil temperature [118–120], leading to distinct negative biases in winter time soil temperatures. The association of snow density to snow thermal conductivity is fixed for three of the models, while different schemes are used elsewhere (see Table S2). While many models consider the effects of percolating and refreezing melt water, other meteorological events like rain on snow are not well represented, even though they have been shown to impact permafrost temperatures [62].

3.3 | Vegetation

All models except GFDL-LM4.1 adopt a dynamical global vegetation model (DGVM) approach—as opposed to individual-based statistical and demographic—that relies on PFTs to represent different plant characteristics, where "dynamical" indicates that leaf area index is a prognostic variable. This approach uses

fractional PFT coverage, which allows for a mixture of PFTs within a single grid point, which is critical for capturing vegetation heterogeneity. In contrast, GFDL-LM4.1 uses a cohort-based approach in its vegetation model, representing ecosystem demography and allowing explicit representation of light competition between PFTs as well as disturbance. Actual vegetation dynamics in terms of changes of PFT distributions with time are included in JSBACH, CoLM, and GFDL-LM4.1. Table S3 presents the variations in PFT utilized by each model for grid points designated as vegetated. Regarding PFTs associated with arctic vegetation used by the models, only five LSMs employ similar Arctic-based PFTs: CLM5, CoLM, ISBA, ELMv0, and JSBACH account for Arctic vegetation through C3 grass and boreal forest PFTs. JSBACH uses a "tundra" PFT, which bears similarities to C3 grass but with a reduced maximum rate of carboxylation in leaves [32]. However, the tundra biome is much more diverse than C3 grass alone, containing a wide variety of shrubs, sedges, mosses, and lichens. Recent work by Sulman et al. [121] and Curasi et al. [122] emphasizes that the addition of new PFTs to represent northern vegetation enhances the ability of LSMs in simulating the carbon cycle over the Arctic region. Rogers et al. [123] point out that implementing trait values observed from Arctic plants is crucial to an accurate representation of photosynthesis in Arctic PFTs implemented in models. Snow vegetation interaction discussed in relevance for permafrost mainly focuses on changes in snow thermal conductivity considering different vegetation buried in snow as well as different snowpack properties associated with vegetation (boreal forest and shrubs) [124]. To be able to consider these processes, LSMs need to represent shrubs as PFTs (see Table S3) as well as employ dynamic snow thermal conductivity schemes (see Table S2). From the models containing both capabilities, only SURFEX employing CROCUS has the capability to consider shrub–snow interactions by modifying snow compaction depending on the vegetation type [125].

3.4 | Wetlands

While the representation of wetlands in LSMs differs considerably among models, most models employ dynamic wetland

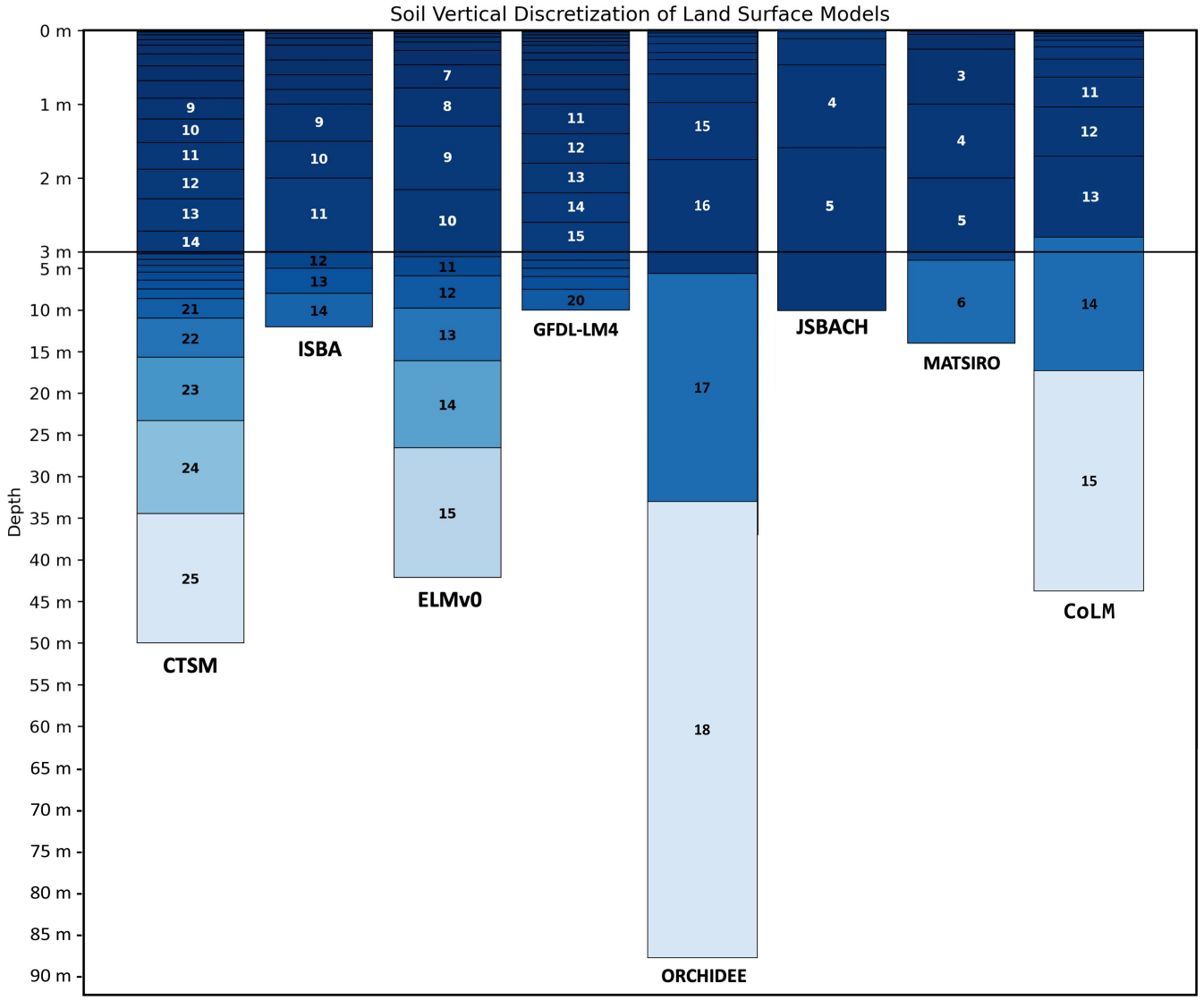

FIGURE 1 | Overview of column structures in LSMs of CMIP6 models fulfilling the selection criteria. [Colour figure can be viewed at wileyonlinelibrary.com]

TABLE 2 | Soil physical characteristics of land surface models.

LSM	Max no layers (max depth)	Latent heat included	Soil heat capacity scheme	Soil thermal conductivity scheme	Organic carbon included	Soil hydrology parametrization
CLM5	20 soil + 5 bedrock layers (50 m)	Yes	de Vries [109]	Lawrence and Slater [47]	Yes	Richards equations (BC model)
SURFEX	14 soil layers (12 m)	Yes	de Vries [109]	Peters-Lidard et al. [110]	Yes	Mixed form of Richards equation (BC or VG model)
ELMv0	15 soil layers (42.1 m)	Yes	de Vries [109]	Lawrence and Slater [47]	Yes	Richards equations (BC model)
GFDL-LM4.1	20 soil layers (10 m)	Yes	Fixed, depending on soil type	Fixed depending on soil type	Yes	Continuous vertical representation of soil water including water table depth
ORCHIDEE	32 soil layers (87 m)—soil hydrology only in 11 layers (2 m)	No	de Vries [109]	Wang, Cheruy, and Dufresne [111]	Yes	Richards equations (VG model)
MATSIRO6.0	6 soil layers (14 m)	No	Saito [112]	Sass, Lachenbruch, and Munroe [113]	Yes	Richards equations (BC model)
CoLM	15 soil layers (44 m)	Yes	de Vries [109]	Farouki [114]	Yes	Richards equations (BC model)
JSBACH	5 (7) soil layers (10 m (30.1 m))	No	de Vries [109]	Johansen [115]	Yes	Richards equations (VG model)

schemes. Wetland extent is determined using water table depth or saturated soil in combination with soil properties (CLM5, Lawrence et al. [41]) or subgrid-scale orography parameters (ORCHIDEE, Ringeval et al. [126]). MATSIRO employs predetermined wetland areas for the high latitudes [127], SURFEX also uses a fixed wetland map that is represented as a landcover type [128], and wetlands in CoLM are also based on a fixed wetland map. GFDL LM4.1 and JSBACH3.2 have no explicit wetland representation. The wetland schemes in all models do not represent ice wedges or other forms of excess ice or talik formation associated with open water bodies.

4 | What Processes/Parameterizations Are LSMs Coupled to ESMs Working on?

Various LSMs discussed above have worked on improvements in the representation of physical processes that impact permafrost since their CMIP6 simulations were completed. The following section summarizes model developments regarding processes relevant to permafrost dynamics. To assess these developments, we conducted a literature review focused on publications that referred to model versions that extended the CMIP6 contributions of the coupled ESMs. We acknowledge that this section can only give an overview of potential model developments going towards the next phase of ESM simulations for CMIP7, since not all of the LSM developments might be incorporated into the coupled frameworks of their parent ESMs. Furthermore, the conclusions drawn from offline simulations of LSMs in terms of model performance for specific process representations are in their direct implications restricted to these offline simulations. Implementing the same changes in coupled ESM simulations might yield different performance results, for example, because of the LSM's sensitivity to meteorological forcing (see, for example, Hardouin et al. [129]).

The Community Land Model 6 (CLM6) has integrated a subgrid-scale hillslope hydrology scheme [73], improved their snow albedo model [130], and included means to change the parameterization used for snow thermal conductivity (following findings in [119]). New surface datasets will provide updates to soil properties, including organic matter contents that are used in global simulations. Ongoing parameter calibration activities are aimed at increasing vegetation survival in permafrost regions, relative to previous versions of the model [131].

CLASS/CTEM already contains representation of latent heat of freeze and thaw and organic matter in the soil column, one snow layer considering snow densification by compaction and refreezing, dynamical vegetation, and a dynamical wetland representation based on soil water content and subgrid-scale orography (Swart et al. [98], Verseghy [132], Verseghy [133], Arora, Melton, and Plummer [134]). CLASSIC1.0 [135] is the successor of CLASS/CTEM and has implemented a wide array of improvements concerning permafrost processes [136], for example, a much deeper soil column (61.4 m), a more complex snow aging, shrubs [137], and nitrogen cycling [138]. Furthermore, CLASSIC1.0 has been expanded to contain PFTs representative of the Canadian Arctic [122] and is indicated to improve the simulation of permafrost carbon dynamics by replacing its bulk soil carbon pool with an explicit tracking of soil carbon per soil layer ([135].

ICON-ESM V1.0 [139], which comprises a part of the JSBACH model (JSBACH v 4.3, [101]) now called ICON-LAND, was represented only in the historical simulations in CMIP6 and, therefore, not discussed above. It includes moisture phase transitions, the representation of supercooled water, and an improved snow scheme [140]. Updates to the computation of soil thermal properties were made considering the amount of water, ice, and organic content within the soil. The current ICON release (2024.07) contains further enhancements to the soil hydrology scheme, including vertical variations in organic matter content that dynamically affect thermal and hydrological soil properties. The presence of ice modulates the vertical soil water transport, and the root zone is confined to the depth of the active layer, leading to a more plausible representation of plant water stress in the boreal regions.

Advancements in ORCHIDEE now enable the incorporation of processes related to the generation, movement, and emission of dissolved organic carbon (DOC) from permafrost soils in high-latitude regions to inland waters and the ocean [141]. A representation of hillslope hydrology [142] has been implemented, albeit in a version where permafrost was turned off. The peatland representation [143] was extended to allow the computation of methane emissions from northern peatlands, tested in single-site simulations [144].

For GFDL-LM4.1, a new snow scheme has been developed [145], which has a dynamical vertical snow structure, accounting for the temporal development of snow grain size and shape. This new scheme has impacts on bulk snow properties such as depth, thermal conductivity, and optical characteristics. Comparisons with previous versions of the GFDL snow model reveal the improved scheme enhances predictions of seasonal snow water equivalent and soil temperature beneath the snowpack.

LPJ-GUESS has recently been extended to contain a standard 3 m, nine-layer soil column in its setup within the EC-Earth model [146]. The representation of soil physical processes was also modified in general, and soil heat transport is now calculated by solving the heat diffusion equation, while soil water transport is solved by applying Richards' equation. LPJ-GUESS can now also be run with a multilayer snow model [57].

JULES has been enabled to represent subgrid-scale microtopography highly prevalent in the permafrost landscapes through a tiling approach [147]. There is also work towards enabling soil heterogeneity at the subgrid-scale level [148]. Offline versions of JULES have been run with deeper soil layers, a representation of organic soil properties, and an additional thermal column at the base of the soil profile to represent bedrock [149]. An interactive nitrogen cycle has been included, showing the impact of thawing permafrost fertilizing the vegetation [150].

CoLM includes carbon–nitrogen interactions, supercooled liquid water in the soil column, and a multilayer soil organic carbon (OC) scheme for cryoturbation and bioturbation allowing soil carbon generated at the top of the soil column to propagate downwards [151].

5 | Where Do the Offline Models Stand and What Are Potential Synergies in Developments?

Offline permafrost models are not part of a coupled Earth System modeling framework. They are generally forced by near-surface meteorological variables, for example, air temperature, precipitation, and relative humidity, which can be obtained from measurements, historical climate datasets, or atmospheric model projections. These forcing data are static and not influenced by the state of the land surface. While this may introduce inconsistencies, offline models offer distinct advantages in many applications.

Offline permafrost models are free of the operational burdens of a comprehensive ESM which offers developers more freedom and allows for rapid innovation cycles. A simpler regional or local application reduces restrictions on horizontal resolution. Forcing models with observed meteorological data, as opposed to the modeled climate in a coupled ESM, removes potential biases in the atmospheric model and interactive feedback between components of the coupled systems that may accentuate these biases. The same development cycles can be employed in LSMs that are components of ESMs, when the models are used in an "offline" configuration outside of the coupled ESM.

There are a large number of offline permafrost models, developed with different purposes in mind. Equilibrium models are widely used to determine permafrost maps, for example, CryoGrid1 for Scandinavia [152] or GIPL1 for Alaska [153]. For assessments of climate change on permafrost extent and active layer development, spatial numerical models solving the surface energy balance like CryoGrid3 (e. g., [154]), GIPL2 (e. g., [155]), the CoupModel (e. g., [156]), or GEOtop2.0 (e. g., [157]) have been applied. Cold-region hydrological models with a focus on permafrost-associated hydrological changes have been used equally widely, including WASIM [158], TopoFlow [159], SUTRA-ICE [160], permaFoam [161], PFLOTRAN-Ice [162], and Amanzi-ATS [163, 164]; see Bui, Lu, and Nie [165] for an overview. Some of these models (PFLOTRAN, SUTRA, and ATS) are high-fidelity models that were developed to study small watershed-type regions. On the large grid cells commonly used in ESMs, their representation of hydrological processes would largely be on the subgrid-scale level. To run these models on larger regions (Alaska, Norway, etc.) would be impractical and impossible due to massive computational demand.

The flexibility of offline models facilitates fast development cycles and allows for the exploration of new parameterizations and enhanced model components. An example is the subsurface grid structure and maximum depth which is generally fixed in coupled models due to computational constraints, while it can be selected completely free in most offline models (e.g., [166]). As a result, ground thermal properties can be calibrated for different ecosystems and upscaled using local or regional landcover maps and data assimilation from site-level field observations [167]. Similar to some LSMs in coupled frameworks, offline models can also represent the physical properties of multiple organic horizons and represent the dynamic of organic layer thickness resulting from litterfall and decomposition, disturbances such as wildfire, or vegetation succession. Thus, these models can directly represent the impact of the organic layer composition and dynamic on permafrost vulnerability to thaw in response to wildfire or climate warming [168–170]. In the past years, successful algorithms first demonstrated in offline models have found their way into land-surface schemes of ESMs. An example is a representation of excess ice melt in complex microtopography, in particular polygonal tundra and peat plateaus. Developed first in the offline permafrost model CryoGrid [171], the algorithm was adapted and implemented for offline NOAH-MP simulations [172] and offline JULES simulations [147], potentially being included in their parent ESMs (IITM-ESM for NOAH-MP and HadGEM, KACE, and UKESM for JULES).

Offline models also offer the advantage that, while they inherently solve conservation equations for mass, carbon, and energy, they are not constrained by the strict coupling requirements of ESMs. This flexibility allows for easier experimentation and development, as any conservation issues that arise do not disrupt the functioning of the broader modeling system, unlike in fully coupled ESMs where violations of conservation can cause the entire system to fail. This freedom allows for more detailed examination of small-scale processes and their impact on permafrost dynamics (e.g. [173]), but it also limits the possibilities of integrating developments into ESM frameworks.

On spatial scales of meters to hundreds of meters, offline permafrost models enable spatially distributed modeling of key landscape-scale processes, for example, related to ground ice and the water cycle [174]. In particular, models like Amanzi-ATS and CryoGrid3 have variable vertical structuring that allows explicit representation of ground ice dynamics, melt ponds, subsidence, and microtopography as well as water flow [166, 174]. By considering the heterogeneity and microtopography of the terrain at a meter or even submeter lateral resolution, dedicated offline models can simulate the spatial variation in properties and processes affecting the ground thermal regime, both in natural settings (e.g., [175, 176]) and around infrastructure elements [152]. This capability is crucial for accurately representing the complexity of permafrost regions, where variations in soil properties, ground ice, vegetation cover, and microtopography significantly influence permafrost dynamics (e.g. [45, 177]). This allows the representation of effects like differential subsidence caused by the melting of excess ground ice leading to significant drying on decadal timescales [174], which LSMs in ESMs cannot capture. High-resolution simulations with offline permafrost models can also be directly compared to laboratory experiments, site-scale observations, or catchment-scale observations, to analyze model performance and parameter uncertainties [174, 178]. Bui, Lu, and Nie [165] provide a review on offline hydrological models for the Arctic permafrost region, discussing the applicability on different spatial scales (e.g., small-scale catchments versus large-scale catchments) as well as cryohydrological process representation. They find that different models have strengths on different scales, stating that "GEOtop, SUTRA-ICE, and PFLOTRAN-ICE are found to be suitable for small-scale catchments, whereas ATS and CryoGrid3 are potentially suitable for large-scale catchments."

Offline permafrost models also have fewer constraints on runtime compared to their coupled counterparts. In global-scale Earth system and even regional circulation models, computational resources are distributed among various components,

constraining the spatial extent of the simulations to global or large regions and limiting the spatiotemporal resolution at which simulations are conducted. In contrast, offline models can concentrate computational resources on specific regions of interest. This not only enables higher resolution simulations of permafrost dynamics (e.g., [179]) but also simulations of permafrost dynamics on centennial to millennial timescales, allowing for the representation of the legacy effect of past climate on current and future permafrost distribution (e.g., [180–182]).

In particular, offline models can also be forced by a simple temperature boundary condition for spatially explicit simulations of permafrost mapping using near-surface air or surface temperature. Regional air temperature data sets at kilometer-scale resolutions have been used to generate permafrost maps with offline models (e.g., [155, 183, 184]), while globally available satellite-derived land surface temperatures were ingested in an empirical offline model to produce a northern hemisphere permafrost map at 1-km scale [185]. In summary, the flexibility of offline models broadens our toolbox for permafrost investigations and enhances our understanding of complex interactions between permafrost and the Earth system.

6 | Discussion: Advancements and Challenges in Permafrost Representation Within ESMs

A number of challenges in land surface modeling in general (e.g., [26, 27]) as well as in the representation of permafrost-related processes in Earth system modeling [22, 186] have been identified and discussed in the past years, suggesting development priorities for improving model projections of Earth's climate as well as giving recommendations on how to tackle open questions. The vast majority of models assessed in this study (57 out of 64) employ sophisticated, well-documented LSMs that can potentially address these challenges. Among these models, we identified two different approaches to implementing advancements in LSMs into ESMs: 41 out of the 64 models listed in Table S1 employ LSMs that are also developed outside their ESMs as stand-alone models, often by modeling groups associated with the same modeling center as the ESM. A second method used for the integration of LSMs into ESMs is to utilize an externally developed, complex LSM, which is used by 16 models.

ESMs from the first group benefit from developments of their LSMs outside of the coupled ESM framework, for example, in applications like ISIMIP [187]. Many of these LSMs have made headway towards the recommendations for better representation of permafrost-related processes since their CMIP6 ScenarioMIP simulations were completed. In concurrence, a number of these LSMs can be run with varying levels of complexity, where the application of a more complex setting than what was used for CMIP6 would already allow them to address some of the recommendations and requirements made with respect to permafrost-relevant processes. For example, SURFEX can be run with the sophisticated snow model CROCUS [59] which has improved capabilities of representing the interaction between Arctic vegetation and snow [118]. NOAH-MP, LPJ-GUESS, JSBACH, JULES, CLASSIC, and CLM5 can be run with varying numbers of soil layers covering requirements like high resolution in the upper soil column as well as sufficiently deep overall soil columns. CLM and ELM can be run with the ecosystem dynamics model FATES in an offline configuration [188] instead of the standard DGVM big leaf scheme. Adjusting the level of complexity of the LSMs employed in coupled ESM simulations can improve the capacity for permafrost representation in coupled ESMs; however, technical and computational constraints often limit the complexity of LSMs applied in coupled ESM simulations. Additionally, within ESMs, the computing infrastructure is often not set up to handle lateral exchange between grid cells, a logistical challenge that offline permafrost models developed as hydrological models have addressed already, but limited to small regional extents like watersheds. Integrating lateral transport into LSMs that are applied to large domains is limited by computational constraints.

The group of models utilizing externally developed, complex LSMs can also directly benefit from the developments in their employed LSM regarding permafrost processes or from employing more complex setups of the LSMs they incorporate than they did within the CMIP6 ScenarioMIP framework. However, ESMs using externally developed LSMs may not have the same depth of understanding of the model as groups that develop their LSMs in-house. This could potentially limit their ability to fully leverage new scientific advances or functionalities. Nonetheless, external LSMs are often accompanied by extensive documentation, user support, and ongoing collaborations with development teams, which help mitigate these limitations and enable meaningful integration of advanced processes into the ESMs. For example, among the 17 models in this group, 11 models use some version of CLM, either the most recent version within the CMIP6 framework (CLM5, in NorESM), older versions (CLM4.0 or CLM4.5 in CMCC-CM2-SR5, CMCC-ESM 2, FGOALS-f3-L, FIO-ESM-2-0, KIOST-ESM, SAM0-UNICON, and TaiESM1), or modified versions of CLM4.5 (CIESM and FGOALS-g3). While updating model versions in a coupled framework poses a multitude of technical challenges and does not always directly yield improvements of the coupled simulations (like the improvement of process representation in general; see e.g., [189, 190]), the capability of the models using older versions of CLM to represent permafrost dynamics could be improved by incorporating the most recent CLM developments. Similar to the ESMs with a direct involvement in “their” LSM development, ESMs could improve their permafrost process representation by including a higher level of complexity in the LSM. For example, as apparent from Table S1, various ESMs using development versions of CLM employ the “BGC mode,” which allows for terrestrial carbon cycling, but most do not, even though this capability existed already in CLM4 [191].

The remaining group of 7 ESMs employs land surface schemes not well documented and often less complex. These models may have other development priorities, potentially in combination with limited resources, or difficulty acquiring expertise in land surface modeling. However, even among that group of ESMs, several modeling groups have made significant progress in representing permafrost-related processes in comparison to CMIP5 (HAL and INM-LND1).

Overall, the advancements made in offline versions of LSMs and offline permafrost models provide valuable insights that can be

incorporated into coupled ESMs to enhance their permafrost representation. However, the implementation is often challenging due to the complex interactions between all components of ESMs, where the improved physical representation of specific processes does not always yield overall improvements in the coupled simulations (e.g., [190]).

7 | Conclusion: Advancing Permafrost Representation in ESMs

In conclusion, while considerable strides have been made in incorporating permafrost dynamics into coupled ESMs, a number of challenges persist. One notable achievement since CMIP5 is the improved understanding of large-scale processes governing permafrost behavior and gradual thaw processes associated with climate change through deeper and better structured soil columns. Yet, fine-scale processes crucial for the accurate representation of permafrost remain inadequately addressed. Here, the challenges arise from the complexity of interactions between thermal and hydrological processes and the high heterogeneity of permafrost landscapes, particularly in remote permafrost regions where data availability is limited and the still often coarse resolution of LSMs in ESMs.

Improving model resolution and complexity, especially through the incorporation of subgrid-scale processes, emerges as a critical pathway towards capturing the heterogeneity of permafrost landscapes. Increasing the spatial resolution to account for microtopography and vegetation patterns, alongside the incorporation of more complex soil columns and lateral processes such as subsurface hydrology, holds the potential for refining permafrost representation. However, this endeavor is hindered by challenges associated with computational costs and the need for better datasets for model initialization and validation at finer scales.

Emphasizing the importance of correct representation of biogeophysical processes as a precursor to accurate biogeochemical process representation underscores the need for continued research and collaboration. Despite existing shortcomings, particularly concerning abrupt thaw processes, current models possess capabilities that can be leveraged for further advancements. Offline permafrost models are important tools to test the influence of the processes driving permafrost dynamics (e.g., lateral flows, dynamic organic layers, and disturbances) and provide information on prioritizing permafrost-related developments in ESMs.

Data Availability Statement

The authors have nothing to report.

References

1. P. Chylek, C. Folland, J. D. Klett, et al., "Annual Mean Arctic Amplification 1970–2020: Observed and Simulated by CMIP6 Climate Models," *Geophysical Research Letters* 49, no. 13 (2022): e2022GL099371.

2. M. Rantanen, A. Y. Karpechko, A. Lipponen, et al., "The Arctic Has Warmed Nearly Four Times Faster Than the Globe Since 1979," *Communications Earth & Environment* 3, no. 1 (2022): 168.

3. B. K. Biskaborn, S. L. Smith, J. Noetzli, et al., "Permafrost Is Warming at a Global Scale," *Nature Communications* 10, no. 1 (2019): 264.

4. A. D. McGuire, D. M. Lawrence, C. Koven, et al., "Dependence of the Evolution of Carbon Dynamics in the Northern Permafrost Region on the Trajectory of Climate Change," *Proceedings of the National Academy of Sciences* 115, no. 15 (2018): 3882–3887.

5. K. R. Miner, M. R. Turetsky, E. Malina, et al., "Permafrost Carbon Emissions in a Changing Arctic," *Nature Reviews Earth and Environment* 3, no. 1 (2022): 55–67.

6. Z. P. Yang, Y. H. Ou, X. L. Xu, L. Zhao, M. H. Song, and C. P. Zhou, "Effects of Permafrost Degradation on Ecosystems," *Acta Ecologica Sinica* 30, no. 1 (2010): 33–39.

7. J. Hjort, O. Karjalainen, J. Aalto, et al., "Degrading Permafrost Puts Arctic Infrastructure at Risk by mid-Century," *Nature Communications* 9, no. 1 (2018): 5147.

8. T. Schneider von Deimling, H. Lee, T. Ingeman-Nielsen, et al., "Consequences of Permafrost Degradation for Arctic Infrastructure – Bridging the Model gap Between Regional and Engineering Scales," *Cryosphere* 15 (2021): 2451–2471.

9. M. Langer, T. S. von Deimling, S. Westermann, et al., "Thawing Permafrost Poses Environmental Threat to Thousands of Sites With Legacy Industrial Contamination," *Nature Communications* 14, no. 1 (2023): 1721.

10. C. M. Gibson, T. Brinkman, H. Cold, D. Brown, and M. Turetsky, "Identifying Increasing Risks of Hazards for Northern Land-Users Caused by Permafrost Thaw: Integrating Scientific and Community-Based Research Approaches," *Environmental Research Letters* 16, no. 6 (2021): 064047.

11. J. Ramage, L. Jungsberg, S. Wang, S. Westermann, H. Lantuit, and T. Heleniak, "Population Living on Permafrost in the Arctic," *Population and Environment* 1-17 (2021): 22–38.

12. G. Hugelius, J. Strauss, S. Zubrzycki, et al., "Estimated Stocks of Circumpolar Permafrost Carbon With Quantified Uncertainty Ranges and Identified Data Gaps," *Biogeosciences* 11, no. 23 (2014): 6573–6593.

13. L. Schirrmeister, G. Grosse, S. Wetterich, et al., "Fossil Organic Matter Characteristics in Permafrost Deposits of the Northeast Siberian Arctic," *Journal of Geophysical Research – Biogeosciences* 116, no. G2 (2011): G00M02, https://doi.org/10.1029/2011JG001647.

14. J. Strauss, L. Schirrmeister, K. Mangelsdorf, L. Eichhorn, S. Wetterich, and U. Herzschuh, "Organic-Matter Quality of Deep Permafrost Carbon–a Study From Arctic Siberia," *Biogeosciences* 12, no. 7 (2015): 2227–2245.

15. Y. K. Vasil'chuk and A. C. Vasil'chuk, "Validity of Radiocarbon Ages of Siberian Yedoma," *GeoResJ* 13 (2017): 83–95.

16. S. M. Natali, J. P. Holdren, B. M. Rogers, et al., "Permafrost Carbon Feedbacks Threaten Global Climate Goals," *Proceedings of the National Academy of Sciences* 118, no. 21 (2021): e2100163118.

17. E. A. Schuur, B. W. Abbott, R. Commane, et al., "Permafrost and Climate Change: Carbon Cycle Feedbacks From the Warming Arctic," *Annual Review of Environment and Resources* 47 (2022): 343–371.

18. D. Riseborough, N. Shiklomanov, B. Etzelmüller, S. Gruber, and S. S. Marchenko, "Recent Advances in Permafrost Modelling," *Permafrost and Periglacial Processes* 19 (2008): 137–156.

19. C. D. Koven, W. J. Riley, and A. Stern, "Analysis of Permafrost Thermal Dynamics and Response to Climate Change in the CMIP5 Earth System Models," *Journal of Climate* 26, no. 6 (2013): 1877–1900.

20. K. E. Taylor, R. J. Stouffer, and G. A. Meehl, "An Overview of CMIP5 and the Experiment Design," *Bulletin of the American Meteorological Society* 93, no. 4 (2012): 485–498.

21. A. D. McGuire, D. J. Hayes, D. W. Kicklighter, et al., "An Analysis of the Carbon Balance of the Arctic Basin From 1997 to 2006," *Tellus B: Chemical and Physical Meteorology* 62, no. 5 (2010): 455–474.

22. C. Schädel, B. M. Rogers, D. M. Lawrence, et al., "Earth System Models Must Include Permafrost Carbon Processes," *Nature Climate Change* 14 (2024): 114–116, https://doi.org/10.1038/s41558-023-01909-9.

23. C. G. Andresen, D. M. Lawrence, C. J. Wilson, et al., "Soil Moisture And Hydrology Projections of the Permafrost Region – A Model Intercomparison," *Cryosphere* 14 (2020): 445–459, https://doi.org/10.5194/tc-14-445-2020.

24. G. Hu, L. Zhao, R. Li, et al., "Water and Heat Coupling Processes and Its Simulation in Frozen Soils: Current Status and Future Research Directions," *Catena* 222 (2023): 106844.

25. V. Humphrey, A. Berg, P. Ciais, et al., "Soil Moisture–Atmosphere Feedback Dominates Land Carbon Uptake Variability," *Nature* 592, no. 7852 (2021): 65–69.

26. E. M. Blyth, V. K. Arora, D. B. Clark, et al., "Advances in Land Surface Modelling," *Current Climate Change Reports* 7, no. 2 (2021): 45–71.

27. R. A. Fisher and C. D. Koven, "Perspectives on the Future of Land Surface Models and the Challenges of Representing Complex Terrestrial Systems," *Journal of Advances in Modeling Earth Systems* 12 (2020): e2018MS001453.

28. J. G. Canadell, P. M. S. Monteiro, M. H. Costa, et al., "Global Carbon and Other Biogeochemical Cycles and Feedbacks," in *Climate Change 2021: The Physical Science Basis* (Cambridge, UK: Cambridge University Press, 2021): 673–816.

29. V. Eyring, S. Bony, G. A. Meehl, et al., "Overview of the Coupled Model Intercomparison Project Phase 6 (CMIP6) Experimental Design and Organization," *Geoscientific Model Development* 9, no. 5 (2016): 1937–1958.

30. D. Chen, M. Rojas, B. H. Samset, et al., "Framing, Context, and Methods," in *Climate Change 2021: The Physical Science Basis* (Cambridge, UK: Cambridge University Press, 2021): 147–286.

31. E. Burke, Y. Zhang, and G. Krinner, "Evaluating Permafrost Physics in the Coupled Model Intercomparison Project 6 (CMIP6) Models and Their Sensitivity to Climate Change," *Cryosphere* 14, no. 9 (2020): 3155–3174.

32. S. E. Chadburn, G. Krinner, P. Porada, et al., "Carbon Stocks and Fluxes in the High Latitudes: Using Site-Level Data to Evaluate Earth System Models," *Biogeosciences* 14, no. 22 (2017): 5143–5169.

33. V. K. Arora, A. Katavouta, R. G. Williams, et al., "Carbon–Concentration and Carbon–Climate Feedbacks in CMIP6 Models and Their Comparison to CMIP5 Models," *Biogeosciences* 17 (2020): 4173–4222.

34. A. Gagné-Landmann, C. Schaedel, J. Wells, et al., "The State of the Art of Modeling Permafrost Carbon Dynamics," *Journal of Geophysical Research – Biogeosciences* forthcoming.

35. Y. Dai, N. Wei, H. Yuan, et al., "Evaluation of Soil Thermal Conductivity Schemes for Use in Land Surface Modeling," *Journal of Advances in Modeling Earth Systems* 11, no. 11 (2019): 3454–3473.

36. H. He, G. N. Flerchinger, Y. Kojima, and M. Dyck, "A Review and Evaluation of 39 Thermal Conductivity Models for Frozen Soils," *Geoderma* 382 (2021): 114694.

37. R. Li, L. Zhao, T. Wu, et al., "Soil Thermal Conductivity and Its Influencing Factors at the Tanggula Permafrost Region on the Qinghai–Tibet Plateau," *Agricultural and Forest Meteorology* 264 (2019): 235–246.

38. M. A. Walvoord and B. L. Kurylyk, "Hydrologic Impacts of Thawing Permafrost—A Review," *Vadose Zone Journal* 15, no. 6 (2016): vzj2016-01.

39. B. Gao and E. T. Coon, "Evaluating Simplifications of Subsurface Process Representations for Field-Scale Permafrost Hydrology Models," *Cryosphere* 16, no. 10 (2022): 4141–4162.

40. J. Bi, L. Li, Z. Liu, Z. Wu, and G. Wang, "Assessment and Enhancement of Soil Freezing Characteristic Curve Estimation Models," *Cold Regions Science and Technology* 218 (2024): 104090.

41. D. M. Lawrence, R. A. Fisher, C. D. Koven, et al., "The Community Land Model Version 5: Description of New Features, Benchmarking, and Impact of Forcing Uncertainty," *J Adv Model Earth Syst.* 11, no. 12 (2019): 4245–4287.

42. V. A. Alexeev, D. J. Nicolsky, V. E. Romanovsky, and D. M. Lawrence, "An Evaluation of Deep Soil Configurations in the CLM3 for Improved Representation of Permafrost: How Deep Should the CLM3 Soil Layer Be?," *Geophysical Research Letters* 34, no. 9 (2007): L09502, https://doi.org/10.1029/2007GL029536.

43. I. Hermoso de Mendoza, H. Beltrami, A. H. MacDougall, and J. C. Mareschal, "Lower Boundary Conditions in Land Surface Models – Effects on the Permafrost and the Carbon Pools: A Case Study With CLM4.5," *Geoscientific Model Development* 13 (2020): 1663–1683.

44. E. Jafarov and K. Schaefer, "The Importance of a Surface Organic Layer in Simulating Permafrost Thermal and Carbon Dynamics," *Cryosphere* 10, no. 1 (2016): 465–475.

45. A. L. Atchley, E. T. Coon, S. L. Painter, D. R. Harp, and C. J. Wilson, "Influences and Interactions of Inundation, Peat, and Snow on Active Layer Thickness," *Geophysical Research Letters* 43, no. 10 (2016): 5116–5123.

46. B. D. Hudson, "Soil Organic Matter and Available Water Capacity," *Journal of Soil and Water Conservation* 49, no. 2 (1994): 5.

47. D. M. Lawrence and A. G. Slater, "Incorporating Organic Soil Into a Global Climate Model," *Climate Dynamics* 30 (2008): 145–160.

48. B. Decharme, E. Brun, A. Boone, C. Delire, P. LeMoigne, and M. Sl, "Impacts of Snow and Organic Soils Parameterization on Northern Eurasian Soil Temperature Profiles Simulated by the ISBA Land Surface Model," *Cryosphere* 10, no. 2 (2016): 853–877.

49. D. Zhu, P. Ciais, G. Krinner, F. Maignan, A. Jornet Puig, and G. Hugelius, "Controls of Soil Organic Matter on Soil Thermal Dynamics in the Northern High Latitudes," *Nature Communications* 10, no. 1 (2019): 3172.

50. A. Rinke, P. Kuhry, and K. Dethloff, "Importance of a Soil Organic Layer for Arctic Climate: A Sensitivity Study With an Arctic RCM," *Geophysical Research Letters* 35, no. 13 (2008): L13709.

51. D. M. Lawrence, A. G. Slater, V. E. Romanovsky, and D. J. Nicolsky, "Sensitivity of a Model Projection of Near-Surface Permafrost Degradation to Soil Column Depth and Representation of Soil Organic Matter," *Journal of Geophysical Research - Earth Surface* 113 (2008): 113(F2).

52. R. Dankers, E. J. Burke, and J. Price, "Simulation of Permafrost and Seasonal Thaw Depth in the JULES Land Surface Scheme," *Cryosphere* 5, no. 3 (2011): 773–790.

53. J. P. Paquin and L. Sushama, "On the Arctic Near-Surface Permafrost and Climate Sensitivities to Soil and Snow Model Formulations in Climate Models," *Climate Dynamics* 44 (2015): 203–228.

54. F. Domine, M. Barrere, and D. Sarrazin, "Seasonal Evolution of the Effective Thermal Conductivity of the Snow and the Soil in High Arctic Herb Tundra at Bylot Island, Canada," *Cryosphere* 10, no. 6 (2016): 2573–2588.

55. G. Li, Y. Zhao, W. Zhang, and X. Cu, "Influence of Snow Cover on Temperature Field of Frozen Ground," *Cold Regions Science and Technology* 192 (2021): 103402.

56. M. Langer, S. Westermann, M. Heikenfeld, W. Dorn, and J. Boike, "Satellite Based Modeling of Permafrost Temperatures in a Tundra Lowland Landscape," *Remote Sensing of Environment* 135 (2013): 12–24.

57. A. Pongracz, D. Wårlind, P. A. Miller, and F.-J. W. Parmentier, "Model Simulations of Arctic Biogeochemistry and Permafrost Extent Are Highly Sensitive to the Implemented Snow Scheme in LPJ-GUESS," *Biogeosciences* 18 (2021): 5767–5787.

58. Y. C. Yen, *Review of Thermal Properties of Snow, Ice, and Sea Ice*, Vol. 81, 1–27 (Hanover, NH: US Army, Corps of Engineers, Cold Regions Research and Engineering Laboratory, 1981).

59. M. Barrere, F. Domine, B. Decharme, S. Morin, V. Vionnet, and M. Lafaysse, "Evaluating the Performance of Coupled Snow-Soil Models in SURFEXv8 to Simulate the Permafrost Thermal Regime at a High Arctic Site," *Geoscientific Model Development* 10, no. 9 (2017): 3461–3479.

60. C. Beer, P. Porada, A. Ekici, and M. Brakebusch, "Effects of Short-Term Variability of Meteorological Variables on Soil Temperature in Permafrost Regions," *Cryosphere* 12 (2018): 741–757.

61. M. R. McCrystall, J. Stroeve, M. Serreze, B. C. Forbes, and J. A. Screen, "New Climate Models Reveal Faster and Larger Increases in Arctic Precipitation Than Previously Projected," *Nature Communications* 12, no. 1 (2021): 6765.

62. K. J. Rennert, G. Roe, J. Putkonen, and C. M. Bitz, "Soil Thermal and Ecological Impacts of Rain on Snow Events in the Circumpolar Arctic," *Journal of Climate* 22, no. 9 (2009): 2302–2315.

63. S. Westermann, J. Boike, M. Langer, T. V. Schuler, and B. Etzelmüller, "Modeling the Impact of Wintertime Rain Events on the Thermal Regime of Permafrost," *Cryosphere* 5, no. 4 (2011): 945–959.

64. J. M. Oehri, G. Schaepman-Strub, J.-S. Kim, et al., "Vegetation Type Is an Important Predictor of the Arctic Summer Land Surface Energy Budget," *Nature Communications* 13 (2022): 6379.

65. J. Beringer, A. H. Lynch, F. S. Chapin, M. Mack, and G. B. Bonan, "The Representation of Arctic Soils in the Land Surface Model: The Importance of Mosses," *Journal of Climate* 14 (2001): 3324–3335.

66. P. Porada, A. Ekici, and C. Beer, "Effects of Bryophyte and Lichen Cover on Permafrost Soil Temperature at Large Scale," *Cryosphere* 10 (2016): 2291–2315.

67. M. R. Turetsky, B. Bond-Lamberty, E. Euskirchen, et al., "The Resilience and Functional Role of Moss in Boreal and Arctic Ecosystems," *New Phytologist* 196, no. 1 (2012): 49–67.

68. P. Y. Bernier, R. L. Desjardins, Y. Karimi-Zindashty, et al., "Boreal Lichen Woodlands: A Possible Negative Feedback to Climate Change in Eastern North America," *Agricultural and Forest Meteorology* 151, no. 4 (2011): 521–528.

69. D. Blok, M. P. D. Heijmans, G. Schaepman-Strub, A. V. Kononov, T. C. Maximov, and F. Berendse, "Shrub Expansion may Reduce Summer Permafrost Thaw in Siberian Tundra," *Global Change Biology* 16 (2010): 1296–1305.

70. G. E. Liston, J. P. McFadden, M. Sturm, and R. A. Pielke, Sr., "Modelled Changes in Arctic Tundra Snow, Energy and Moisture Fluxes due to Increased Shrubs," *Global Change Biology* 8 (2002): 17–32.

71. H. Kropp, M. M. Loranty, S. M. Natali, et al., "Shallow Soils Are Warmer Under Trees and Tall Shrubs Across Arctic and Boreal Ecosystems," *Environmental Research Letters* 16 (2020): 015001.

72. Z. A. Mekonnen, W. J. Riley, L. T. Berner, et al., "Arctic Tundra Shrubification: A Review of Mechanisms and Impacts on Ecosystem Carbon Balance," *Environmental Research Letters* 16, no. 5 (2021): 053001.

73. C. Robinson, P. Roy-Léveillée, K. Turner, and N. Basiliko, "Impacts of Shrubification on Ground Temperatures and Carbon Cycling in a sub-Arctic fen Near Churchill, MB," in *Regional Conference on Permafrost 2021 and the 19th International Conference on Cold Regions Engineering*, (Reston, VA: American Society of Civil Engineers, 2021): 60–70.

74. J. Cohen, J. Pulliainen, C. B. Ménard, et al., "Effect of Reindeer Grazing on Snowmelt, Albedo and Energy Balance Based on Satellite Data Analyses," *Remote Sensing of Environment* 135 (2013): 107–117.

75. M. Sturm, T. Douglas, C. Racine, and G. E. Liston, "Changing Snow and Shrub Conditions Affect Albedo With Global Implications," *Journal of Geophysical Research – Biogeosciences* 110, no. G1 (2005): G01004.

76. I. Grünberg, E. J. Wilcox, S. Zwieback, P. Marsh, and J. Boike, "Linking Tundra Vegetation, Snow, Soil Temperature, and Permafrost," *Biogeosciences* 17 (2020): 4261–4279.

77. M. Sturm, J. Holmgren, J. P. McFadden, G. E. Liston, F. S. Chapin, and C. H. Racine, "Snow–Shrub Interactions in Arctic Tundra: A Hypothesis With Climatic Implications," *Journal of Climate* 14, no. 3 (2001): 336–344.

78. F. Domine, K. Fourteau, G. Picard, G. Lackner, D. Sarrazin, and M. Poirier, "Permafrost Cooled in Winter by Thermal Bridging Through Snow-Covered Shrub Branches," *Nature Geoscience* 15, no. 7 (2022): 554–560.

79. M. Abe, K. Takata, M. Kawamiya, and S. Watanabe, "Vegetation Masking Effect on Future Warming and Snow Albedo Feedback in a Boreal Forest Region of Northern Eurasia According to MIROC-ESM," *Journal of Geophysical Research, [Atmospheres]* 122, no. 17 (2017): 9245–9261.

80. M. R. Turetsky, B. W. Abbott, M. C. Jones, et al., "Carbon Release Through Abrupt Permafrost Thaw," *Nature Geoscience* 13, no. 2 (2020): 138–143.

81. F.-J. W. Parmentier, L. Nilsen, H. Tømmervik, et al., "Rapid Ice-Wedge Collapse and Permafrost Carbon Loss Triggered by Increased Snow Depth and Surface Runoff," *Geophysical Research Letters* 51 (2024): e2023GL108020.

82. J. Nitzbon, M. Langer, L. C. Martin, S. Westermann, T. Schneider von Deimling, and J. Boike, "Effects of Multi-Scale Heterogeneity on the Simulated Evolution of Ice-Rich Permafrost Lowlands Under a Warming Climate," *Cryosphere* 15, no. 3 (2021): 1399–1422.

83. S. Hantson, D. I. Kelley, A. Arneth, et al., "Quantitative Assessment of Fire and Vegetation Properties in Simulations With Fire-Enabled Vegetation Models From the Fire Model Intercomparison Project," *Geoscientific Model Development* 13 (2020): 3299–3318.

84. R. A. Fisher, C. D. Koven, W. R. L. Anderegg, et al., "Vegetation Demographics in Earth System Models: A Review of Progress and Priorities," *Global Change Biology* 24, no. 1 (2017): 35–54.

85. S. C. Swenson, M. Clark, Y. Fan, D. M. Lawrence, and J. Perket, "Representing Intrahillslope Lateral Subsurface Flow in the Community Land Model," *Journal of Advances in Modeling Earth Systems* 11, no. 12 (2019): 4044–4065.

86. Y. Shi, W. Gong, Q. Duan, J. Charles, C. Xiao, and H. Wang, "How Parameter Specification of an Earth System Model of Intermediate Complexity Influences Its Climate Simulations," *Progress in Earth and Planetary Science* 6, no. 46 (2019): 1–18.

87. H. Yan, N. Sun, H. Eldardiry, et al., "Characterizing Uncertainty in Community Land Model Version 5 Hydrological Applications in the United States," *Scientific Data* 10 (2023): 187.

88. P. J. Durack, CMIP6_CVs. v6.2.53.5 (2020). Available at: https://github.com/WCRP-CMIP/CMIP6_CVs (Accessed: 12 January 2024).

89. B. Decharme, C. Delire, M. Minvielle, et al., "Recent Changes in the ISBA-CTRIP Land Surface System for Use in the CNRM-CM6 Climate Model and in Global off-Line Hydrological Applications," *Journal of Advances in Modeling Earth Systems* 11 (2019): 1207–1252.

90. J. Golaz, P. M. Caldwell, L. P. Van Roekel, et al., "The DOE E3SM Coupled Model Version 1: Overview and Evaluation at Standard Resolution," *Journal of Advances in Modeling Earth Systems* 11, no. 7 (2019): 2089–2129.

91. M. Zhao, J.-C. Golaz, I. M. Held, et al., "The GFDL Global Atmosphere and Land Model AM4.0/LM4.0: 2. Model Description, Sensitivity Studies, and Tuning Strategies," *Journal of Advances in Modeling Earth Systems* 10, no. 3 (2018): 735–769.

92. E. Shevliakova, S. Malyshev, I. Martinez-Cano, et al., "The Land Component LM4. 1 of the GFDL Earth System Model ESM4. 1: Model Description and Characteristics of Land Surface Climate and Carbon

Cycling in the Historical Simulation," *Journal of Advances in Modeling Earth Systems* 16, no. 5 (2024): e2023MS003922.

93. M. Guimberteau, D. Zhu, F. Maignan, et al., "ORCHIDEE-MICT (v8.4.1), a Land Surface Model for the High Latitudes: Model Description and Validation," *Geoscientific Model Development* 11, no. 1 (2018): 121–163.

94. C. H. Reick, V. Gayler, D. Goll, et al., "JSBACH 3 - The Land Component of the MPI Earth System Model: Documentation of Version 3.2," *Berichte zur Erdsystemforschung* 240 (2021), https://doi.org/10.17617/2.3279802.

95. T. Yokohata, K. Saito, K. Takata, et al., "Model Improvement and Future Projection of Permafrost Processes in a Global Land Surface Model," *Progress in Earth and Planetary Science* 7 (2020): 1–12.

96. Y. Dai, X. Zeng, R. E. Dickinson, et al., "The Common Land Model (CLM)," *Bulletin of the American Meteorological Society* 84 (2003): 1013–1023, https://doi.org/10.1175/BAMS-84-8-1013.

97. C. Li, H. Lu, K. Yang, et al., "Evaluation of the Common Land Model (CoLM) From the Perspective of Water and Energy Budget Simulation: Towards Inclusion in CMIP6," *Atmosphere* 8, no. 8 (2017): 141.

98. N. C. Swart, J. N. S. Cole, V. V. Kharin, et al., "The Canadian Earth System Model Version 5 (CanESM5. 0.3)," *Geoscientific Model Development* 12 (2019): 4823–4873.

99. C. Mathison, E. Burke, A. J. Hartley, et al., "Description and Evaluation of the JULES-ES Set-Up for ISIMIP2b," *Geoscientific Model Development* 16, no. 14 (2023): 4249–4264.

100. A. J. Wiltshire, M. C. Duran Rojas, J. M. Edwards, et al., "JULES-GL7: The Global Land Configuration of the Joint UK Land Environment Simulator version 7.0 and 7.2," *Geoscientific Model Development* 13 (2020): 483–505, https://doi.org/10.5194/gmd-13-483-2020.

101. R. Schneck, V. Gayler, J. E. Nabel, T. Raddatz, C. H. Reick, and R. Schnur, "Assessment of JSBACHv4.30 as a Land Component of ICON-ESM-V1 in Comparison to Its Predecessor JSBACHv3.2 of MPI-ESM 1.2," *Geoscientific Model Development* 15, no. 22 (2022): 8581–8611.

102. C. He, P. Valayamkunnath, M. Barlage, et al., *The Community Noah-MP Land Surface Modeling System Technical Description Version 5.0* (No. NCAR/TN-575+STR) (Boulder, CO: NCAR Tech Note, 2023).

103. V. Haverd, B. Smith, L. Nieradzik, et al., "A New Version of the CABLE Land Surface Model (Subversion Revision r4601) Incorporating Land Use and Land Cover Change, Woody Vegetation Demography, and a Novel Optimisation-Based Approach to Plant Coordination of Photosynthesis," *Geoscientific Model Development* 11 (2018): 2995–3026.

104. T. Wu, L. Song, W. Li, et al., "An Overview of BCC Climate System Model Development and Application for Climate Change Studies," *Journal of Meteorological Research* 28 (2014): 34–56.

105. B. Smith, D. Wårlind, A. Arneth, et al., "Implications of Incorporating N Cycling and N Limitations on Primary Production in an Individual-Based Dynamic Vegetation Model," *Biogeosciences* 11 (2014): 2027–2054.

106. M. Kelley, G. A. Schmidt, L. S. Nazarenko, et al., "GISS-E2.1:Configurations and Climatology," *Journal of Advances in Modeling Earth Systems* 12 (2020): e2019MS002025.

107. S. Yukimoto, H. Yoshimura, M. Hosaka, et al., "Meteorological Research Institute-Earth System Model Version 1 (MRI-ESM 1) -Model Description," *Technical Reports of the Meteorological Research Institute* 64 (2011).

108. E. M. Volodin, E. V. Mortikov, S. V. Kostrykin, et al., "Simulation of the Present-Day Climate With the Climate Model INMCM5," *Climate Dynamics* 49 (2017): 3715–3734.

109. D. de Vries, "Thermal Properties of Soils," in *Physics of the Plant Environment*, eds. W. R. Wijk and A. J. W. Borghorst (Amsterdam, The Netherlands: North-Holland, 1963): 210–235.

110. C. D. Peters-Lidard, E. Blackburn, X. Liang, and E. F. Wood, "The Effect of Soil Thermal Conductivity Parameterization on Surface Energy Fluxes and Temperatures," *Journal of the Atmospheric Sciences* 55, no. 7 (1998): 1209–1224.

111. F. Wang, F. Cheruy, and J.-L. Dufresne, "The Improvement of Soil Thermodynamics and its Effects on Land Surface Meteorology in the IPSL Climate Model," *Geoscientific Model Development* 9, no. 1 (2016): 363–381.

112. K. Saito, "Arctic Land Hydrothermal Sensitivity Under Warming: Idealized Offline Evaluation of a Physical Terrestrial Scheme in a Global Climate Model," *Journal of Geophysical Research* 113, no. D21 (2008): D21106.

113. J. H. Sass, A. H. Lachenbruch, and R. J. Munroe, "Thermal Conductivity of Rocks From Measurements on Fragments and its Application to Heat-Flow Determinations," *Journal of Geophysical Research* 76, no. 14 (1971): 3391–3401.

114. O. T. Farouki, "The Thermal Properties of Soils in Cold Regions," *Cold Regions Science and Technology* 5, no. 1 (1981): 67–75.

115. O. Johansen, *Thermal Conductivity of Soils: Technical report* (Fort Belvoir, VA: Defense Technical Information Center, 1975).

116. R. H. Brooks and A. T. Corey, "Properties of Porous Media Affecting Fluid Flow," *Journal of the Irrigation and Drainage Division* 92, no. 2 (1966): 61–88.

117. M. T. Van Genuchten, "A Closed-Form Equation for Predicting the Hydraulic Conductivity of Unsaturated Soils," *Soil Science Society of America Journal* 44, no. 5 (1980): 892–898.

118. A. Royer, G. Picard, C. Vargel, A. Langlois, I. Gouttevin, and M. Dumont, "Improved Simulation of Arctic Circumpolar Land Area Snow Properties and Soil Temperatures," *Frontiers in Earth Science* 9 (2021): 685140.

119. V. R. Dutch, N. Rutter, L. Wake, et al., "Impact of Measured and Simulated Tundra Snowpack Properties on Heat Transfer," *Cryosphere* 16, no. 10 (2022): 4201–4222.

120. I. Gouttevin, M. Langer, H. Löwe, J. Boike, M. Proksch, and M. Schneebeli, "Observation and Modelling of Snow at a Polygonal Tundra Permafrost Site: Spatial Variability and Thermal Implications," *Cryosphere* 12, no. 11 (2018): 3693–3717.

121. B. N. Sulman, V. G. Salmon, C. M. Iversen, A. L. Breen, F. Yuan, and P. E. Thornton, "Integrating Arctic Plant Functional Types in a Land Surface Model Using Above-and Belowground Field Observations," *Journal of Advances in Modeling Earth Systems* 13, no. 4 (2021): e2020MS002396.

122. S. R. Curasi, J. R. Melton, E. R. Humphreys, et al., "Evaluating the Performance of the Canadian Land Surface Scheme Including Biogeochemical Cycles (CLASSIC) Tailored to the pan-Canadian Domain," *Journal of Advances in Modeling Earth Systems* 15 (2023): e2022MS003480.

123. A. Rogers, B. E. Medlyn, J. S. Dukes, et al., "A Roadmap for Improving the Representation of Photosynthesis in Earth System Models," *New Phytologist* 213, no. 1 (2017): 22–42.

124. G. Leonardini, F. Anctil, V. Vionnet, M. Abrahamowicz, D. F. Nadeau, and V. Fortin, "Evaluation of the Snow Cover in the Soil, Vegetation, and Snow (SVS) Land Surface Model," *Journal of Hydrometeorology* 22, no. 6 (2021): 1663–1680.

125. G. Lackner, F. Domine, D. F. Nadeau, M. Lafaysse, and M. Dumont, "Snow Properties at the Forest–Tundra Ecotone: Predominance of Water Vapor Fluxes Even in Deep, Moderately Cold Snowpacks," *Cryosphere* 16, no. 8 (2022): 3357–3373.

126. B. Ringeval, B. Decharme, S. L. Piao, et al., "Modelling sub-Grid Wetland in the ORCHIDEE Global Land Surface Model: Evaluation Against River Discharges and Remotely Sensed Data," *Geoscientific Model Development* 5, no. 4 (2012): 941–962.

127. T. Nitta, K. Yoshimura, and A. Abe-Ouchi, "Impact of Arctic Wetlands on the Climate System: Model Sensitivity Simulations With the MIROC5 AGCM and a Snow-Fed Wetland Scheme," *Journal of Hydrometeorology* 18, no. 11 (2017): 2923–2936.

128. M. Nogueira, C. Albergel, S. Boussetta, et al., "Role of Vegetation in Representing Land Surface Temperature in the CHTESSEL (CY45R1) and SURFEX-ISBA (v8.1) Land Surface Models: A Case Study Over Iberia," *Geoscientific Model Development* 13 (2020): 3975–3993.

129. L. Hardouin, C. Delire, B. Decharme, et al., "Uncertainty in Land Carbon Budget Simulated by Terrestrial Biosphere Models: The Role of Atmospheric Forcing," *Environmental Research Letters* 17, no. 9 (2022): 094033.

130. C. He, M. Flanner, D. M. Lawrence, and Y. Gu, "New Features and Enhancements in Community Land Model (CLM5) Snow Albedo Modeling: Description, Sensitivity, and Evaluation," *Journal of Advances in Modeling Earth Systems* 16 (2024): e2023MS003861.

131. M. S. A. Lambert, H. Tang, K. S. Aas, et al., "Inclusion of a Cold Hardening Scheme to Represent Frost Tolerance Is Essential to Model Realistic Plant Hydraulics in the Arctic–Boreal Zone in CLM5.0-FATES-Hydro," *Geoscientific Model Development* 15 (2022): 8809–8829.

132. D. L. Verseghy, "CLASS—A Canadian Land Surface Scheme for GCMs. I. Soil Model," *International Journal of Climatology* 11, no. 2 (1991): 111–133.

133. D. L. Verseghy, "CLASS—The Canadian Land Surface Scheme (Version 3.4)—Technical Documentation," Internal Report, Climate Research Division, Science and Technology Branch, Environment Canada, Toronto, Ontario, Canada, 2008.

134. V. K. Arora, J. R. Melton, and D. Plummer, "An Assessment of Natural Methane Fluxes Simulated by the CLASS-CTEM Model," *Biogeosciences* 15, no. 15 (2018): 4683–4709, https://doi.org/10.5194/bg-15-4683-2018.

135. J. R. Melton, V. K. Arora, E. Wisernig-Cojoc, et al., "CLASSIC v1.0: The Open-Source Community Successor to the Canadian Land Surface Scheme (CLASS) and the Canadian Terrestrial Ecosystem Model (CTEM) – Part 1: Model Framework and Site-Level Performance," *Geoscientific Model Development* 13, no. 6 (2020): 2825–2850.

136. J. R. Melton, D. L. Verseghy, R. Sospedra-Alfonso, and S. Gruber, "Improving Permafrost Physics in the Coupled Canadian Land Surface Scheme (V.3.6.2) and Canadian Terrestrial Ecosystem Model (V.2.1) (CLASS-CTEM)," *Geoscientific Model Development* 12 (2019): 4443–4467.

137. G. Meyer, E. R. Humphreys, J. R. Melton, A. J. Cannon, and P. M. Lafleur, "Simulating Shrubs and Their Energy and Carbon Dioxide Fluxes in Canada's Low Arctic With the Canadian Land Surface Scheme Including Biogeochemical Cycles (CLASSIC)," *Biogeosciences* 18 (2021): 3263–3283.

138. A. Asaadi and V. K. Arora, "Implementation of Nitrogen Cycle in the CLASSIC Land Model," *Biogeosciences* 18 (2021): 669–706.

139. J. H. Jungclaus, S. J. Lorenz, H. Schmidt, et al., "The ICON Earth System Model Version 1.0," *Journal of Advances in Modeling Earth Systems* 14, no. 4 (2022): e2021MS002813.

140. A. Ekici, C. Beer, S. Hagemann, J. Boike, M. Langer, and C. Hauck, "Simulating High-Latitude Permafrost Regions by the JSBACH Terrestrial Ecosystem Model," *Geoscientific Model Development* 7, no. 2 (2014): 631–647.

141. S. P. Bowring, R. Lauerwald, B. Guenet, et al., "ORCHIDEE MICT-LEAK (r5459), a Global Model for the Production, Transport, and Transformation of Dissolved Organic Carbon From Arctic Permafrost Regions–Part 1: Rationale, Model Description, and Simulation Protocol," *Geoscientific Model Development* 12, no. 8 (2019): 3503–3521.

142. P. F. Arboleda Obando, A. Ducharne, F. Cheruy, et al., "Influence of Hillslope Flow on Hydroclimatic Evolution Under Climate Change," *Earth's Future* 10, no. 9 (2022): e2021EF002613.

143. C. Largeron, G. Krinner, P. Ciais, and C. Brutel-Vuilmet, "Implementing Northern Peatlands in a Global Land Surface Model: Description and Evaluation in the ORCHIDEE High-Latitude Version Model (ORC-HL-PEAT)," *Geoscientific Model Development* 11, no. 8 (2018): 3279–3297.

144. E. Salmon, F. Jégou, B. Guenet, et al., "Assessing Methane Emissions for Northern Peatlands in ORCHIDEE-PEAT Revision 7020," *Geoscientific Model Development* 15 (2022): 2813–2838.

145. E. Zorzetto, S. Malyshev, P. Ginoux, and E. Shevliakova, "A Global Land Snow Scheme (GLASS) v1. 0 for the GFDL Earth System Model: Formulation and Evaluation at Instrumented Sites," *Geoscientific Model Development* 17, no. 19 (2024): 7219–7244.

146. D. Martín Belda, P. Anthoni, D. Wårlind, et al., "LPJ-GUESS/LSMv1.0: A Next-Generation Land Surface Model With High Ecological Realism," *Geoscientific Model Development* 15, no. 17 (2022): 6709–6745.

147. N. D. Smith, E. J. Burke, K. Schanke Aas, et al., "Explicitly Modelling Microtopography in Permafrost Landscapes in a Land Surface Model (JULES vn5. 4_Microtopography)," *Geoscientific Model Development* 15, no. 9 (2022): 3603–3639.

148. H. S. Rumbold, R. J. Gilham, and M. J. Best, "Assessing Methods for Representing Soil Heterogeneity Through a Flexible Approach Within the Joint UK Land Environment Simulator (JULES) at Version 3.4.1," *Geoscientific Model Development* 16, no. 7 (2023): 1875–1886.

149. E. J. Burke, A. Ekici, Y. Huang, et al., "Quantifying Uncertainties of Permafrost Carbon–Climate Feedbacks," *Biogeosciences* 14, no. 12 (2017): 3051–3066.

150. E. Burke, S. Chadburn, and C. Huntingford, "Thawing Permafrost as a Nitrogen Fertiliser: Implications for Climate Feedbacks," *Nitrogen* 3, no. 2 (2022): 353–375.

151. H. Zhang, M. Zhang, J. Jin, et al., "Description and Climate Simulation Performance of CAS-ESM Version 2," *Journal of Advances in Modeling Earth Systems* 12, no. 12 (2020): e2020MS002210.

152. K. Gisnås, B. Etzelmüller, H. Farbrot, T. Schuler, and S. Westermann, "CryoGRID 1.0: Permafrost Distribution in Norway Estimated by a Spatial Numerical Model," *Permafrost and Periglacial Processes* 24 (2013): 2–19.

153. T. Sazonova and V. Romanovsky, "A Model for Regional-Scale Estimation of Temporal and Spatial Variability of Active Layer Thickness and Mean Annual Ground Temperatures," *Permafrost and Periglacial Processes* 14 (2003): 125–139.

154. S. Westermann, M. Langer, J. Boike, et al., "Simulating the Thermal Regime and Thaw Processes of Ice-Rich Permafrost Ground With the Land-Surface Model CryoGrid 3," *Geoscientific Model Development* 9, no. 2 (2016): 523–546.

155. E. E. Jafarov, S. S. Marchenko, and V. E. Romanovsky, "Numerical Modeling of Permafrost Dynamics in Alaska Using a High Spatial Resolution Dataset," *Cryosphere* 6 (2012): 613–624.

156. L. H. Rasmussen, W. Zhang, J. Hollesen, et al., "Modelling Present and Future Permafrost Thermal Regimes in Northeast Greenland," *Cold Regions Science and Technology* 146 (2018): 199–213.

157. J. Beddrich, S. Gupta, B. Wohlmuth, and G. Chiogna, "The Importance of Topographic Gradients in Alpine Permafrost Modeling," *Advances in Water Resources* 170 (2022): 104321.

158. M. V. Debolskiy, V. A. Alexeev, R. Hock, et al., "Water Balance Response of Permafrost-Affected Watersheds to Changes in air Temperatures," *Environmental Research Letters* 16, no. 8 (2021): 084054.

159. S. D. Peckham, M. Stoica, E. Jafarov, A. Endalamaw, and W. R. Bolton, "Reproducible, Component-Based Modeling With TopoFlow, a Spatial Hydrologic Modeling Toolkit," *Earth and Space Science* 4 (2017): 377–394.

160. J. M. McKenzie, C. I. Voss, and D. I. Siegel, "Groundwater Flow With Energy Transport and Water–Ice Phase Change: Numerical

Simulations, Benchmarks, and Application to Freezing in Peat Bogs," *Advances in Water Resources* 30, no. 4 (2007): 966–983.

161. L. Orgogozo, T. Xavier, H. Oulbani, and C. Grenier, "Permafrost Modelling With OpenFOAM®: New Advancements of the permaFoam Solver," *Computer Physics Communications* 282 (2023): 108541.

162. S. Karra, S. L. Painter, and P. C. Lichtner, "Three-Phase Numerical Model for Subsurface Hydrology in Permafrost-Affected Regions (PFLOTRAN-ICE v1.0)," *Cryosphere* 8 (2014): 1935–1950.

163. S. L. Painter, E. T. Coon, A. L. Atchley, et al., "Integrated Surface/Subsurface Permafrost Thermal Hydrology: Model Formulation and Proof-Of-Concept Simulations," *Water Resources Research* 52, no. 8 (2016): 6062–6077.

164. E. Coon, D. Svyatsky, A. Jan, et al., "Advanced Terrestrial Simulator," Computer Software. USDOE Office of Science (SC), Biological and Environmental Research (BER) (SC-23) (2019), https://doi.org/10.11578/dc.20190911.1.

165. M. T. Bui, J. Lu, and L. Nie, "A Review of Hydrological Models Applied in the Permafrost-Dominated Arctic Region," *Geosciences* 10, no. 10 (2020): 401.

166. S. Westermann, T. Ingeman-Nielsen, J. Scheer, et al., "The CryoGrid Community Model (Version 1.0)–a Multi-Physics Toolbox for Climate-Driven Simulations in the Terrestrial Cryosphere," *Geoscientific Model Development* 16, no. 9 (2023): 2607–2647.

167. D. J. Nicolsky, V. E. Romanovsky, S. K. Panda, S. S. Marchenko, and R. R. Muskett, "Applicability of the Ecosystem Type Approach to Model Permafrost Dynamics Across the Alaska North Slope," *Journal of Geophysical Research: Earth Surface* 122, no. 1 (2017): 50–75.

168. H. Genet, A. D. McGuire, K. Barrett, et al., "Modeling the Effects of Fire Severity and Climate Warming on Active Layer Thickness and Soil Carbon Storage of Black Spruce Forests Across the Landscape in Interior Alaska," *Environmental Research Letters* 8, no. 4 (2013): 045016.

169. E. E. Jafarov, V. E. Romanovsky, H. Genet, A. D. McGuire, and S. S. Marchenko, "The Effects of Fire on the Thermal Stability of Permafrost in Lowland and Upland Black Spruce Forests of Interior Alaska in a Changing Climate," *Environmental Research Letters* 8, no. 3 (2013): 035030.

170. S. Yi, A. D. McGuire, E. Kasischke, et al., "A Dynamic Organic Soil Biogeochemical Model for Simulating the Effects of Wildfire on Soil Environmental Conditions and Carbon Dynamics of Black Spruce Forests," *Journal of Geophysical Research – Biogeosciences* 115, no. G4 (2010): G04015.

171. J. Nitzbon, M. Langer, S. Westemann, L. Martin, K. S. Aas, and J. Boike, "Pathways of Ice-Wedge Degradation in Polygonal Tundra Under Different Hydrological Conditions," *Cryosphere* 13, no. 4 (2019): 1089–1123.

172. K. S. Aas, L. Martin, J. Nitzbon, et al., "Thaw Processes in Ice-Rich Permafrost Landscapes Represented With Laterally Coupled Tiles in a Land Surface Model," *Cryosphere* 13, no. 2 (2019): 591–609.

173. L. C. P. Martin, J. Nitzbon, K. S. Aas, B. Etzelmüller, H. Kristiansen, and S. Westermann, "Stability Conditions of Peat Plateaus and Palsas in Northern Norway," *Journal of Geophysical Research - Earth Surface* 124, no. 3 (2019): 705–719.

174. S. L. Painter, E. T. Coon, A. J. Khattak, and J. D. Jastrow, "Drying of Tundra Landscapes Will Limit Subsidence-Induced Acceleration of Permafrost Thaw," *Proceedings of the National Academy of Sciences* 120, no. 8 (2023): e2212171120.

175. L. C. Martin, J. Nitzbon, J. Scheer, et al., "Lateral Thermokarst Patterns in Permafrost Peat Plateaus in Northern Norway," *Cryosphere* 15, no. 7 (2021): 3423–3442.

176. R. B. Zweigel, S. Westermann, J. Nitzbon, et al., "Simulating Snow Redistribution and Its Effect on Ground Surface Temperature at a High-Arctic Site on Svalbard," *Journal of Geophysical Research - Earth Surface* 126, no. 3 (2021): e2020JF005673.

177. E. E. Jafarov, E. T. Coon, D. R. Harp, et al., "Modeling the Role of Preferential Snow Accumulation in Through Talik Development and Hillslope Groundwater Flow in a Transitional Permafrost Landscape," *Environmental Research Letters* 13, no. 10 (2018): 105006.

178. A. Jan, E. T. Coon, and S. L. Painter, "Evaluating Integrated Surface/Subsurface Permafrost Thermal Hydrology Models in ATS (v0. 88) Against Observations From a Polygonal Tundra Site," *Geoscientific Model Development* 13, no. 5 (2020): 2259–2276.

179. J. Fiddes, S. Endrizzi, and S. Gruber, "Large Area Land Surface Simulations in Heterogeneous Terrain Driven by Global Datasets: Application to Mountain Permafrost," *Cryosphere Discussions* 7 (2013): 5853–5887.

180. B. Etzelmüller, H. Patton, A. Schomacker, et al., "Icelandic Permafrost Dynamics Since the Last Glacial Maximum–Model Results and Geomorphological Implications," *Quaternary Science Reviews* 233 (2020): 106236.

181. M. Langer, J. Nitzbon, B. Groenke, et al., "The Evolution of Arctic Permafrost Over the Last 3 Centuries From Ensemble Simulations With the CryoGridLite Permafrost Model," *Cryosphere* 18, no. 1 (2024): 363–385.

182. P. P. Overduin, T. Schneider von Deimling, F. Miesner, et al., "Submarine Permafrost Map in the Arctic Modeled Using 1-D Transient Heat Flux (Supermap)," *Journal of Geophysical Research: Oceans* 124, no. 6 (2019): 3490–3507.

183. J. Czekirda, S. Westermann, B. Etzelmüller, and T. Jóhannesson, "Transient Modelling of Permafrost Distribution in Iceland," *Frontiers in Earth Science* 7 (2019): 130.

184. N. J. Pastick, P. Duffy, H. Genet, et al., "Historical and Projected Trends in Landscape Drivers Affecting Carbon Dynamics in Alaska," *Ecological Applications* 27, no. 5 (2017): 1383–1402.

185. J. Obu, S. Westermann, A. Bartsch, et al., "Northern Hemisphere Permafrost Map Based on TTOP Modelling for 2000–2016 at 1 km2 Scale," *Earth Science Reviews* 193 (2019): 299–316.

186. B. M. Sanderson, B. B. Booth, J. Dunne, et al., "The Need for Carbon-Emissions-Driven Climate Projections in CMIP7," *Geoscientific Model Development* 17, no. 22 (2024): 8141–8172.

187. C. Rosenzweig, N. W. Arnell, K. L. Ebi, et al., "Assessing Inter-Sectoral Climate Change Risks: The Role of ISIMIP," *Environmental Research Letters* 12, no. 1 (2017): 010301.

188. R. A. Fisher, S. Muszala, M. Verteinstein, et al., "Taking off the Training Wheels: The Properties of a Dynamic Vegetation Model Without Climate Envelopes, CLM4. 5 (ED)," *Geoscientific Model Development* 8, no. 11 (2015): 3593–3619.

189. M. Køltzow, "The Effect of a New Snow and Sea Ice Albedo Scheme on Regional Climate Model Simulations," *Journal of Geophysical Research* 112 (2007): D07110.

190. X. Yu, A. Rinke, W. Dorn, et al., "Evaluation of Arctic Sea Ice Drift and Its Dependency on Near-Surface Wind and Sea Ice Conditions in the Coupled Regional Climate Model HIRHAM–NAOSIM," *Cryosphere* 14 (2020): 1727–1746.

191. D. M. Lawrence, K. W. Oleson, M. G. Flanner, et al., "Parameterization Improvements and Functional and Structural Advances in Version 4 of the Community Land Model," *Journal of Advances in Modeling Earth Systems* 3, no. 1 (2011): M03001.

Supporting Information

Additional supporting information can be found online in the Supporting Information section.